

# Supplementary Information: Modeling the assembly of oppositely charged multi-indented lock- and key-particles

Björn Stenqvist<sup>a,\*</sup> and Jérôme J. Crassous<sup>a,b,‡</sup>

## S1 Key parameters of the model

In the following description of the lock and key assembly model,  $\mathbf{L}$  is the center position of a Lock-particle. For any given location around that  $\mathbf{C}$  is the position of the closest cavity center. Furthermore  $\mathbf{R}$  is defined as any point on the rim of that cavity and the bulk part of the Lock-particle. Finally  $\mathbf{K}$  is the center position of the a Key-particle.

## S2 Entropic contribution

### S2.1 Single cavity

The free energy  $\Delta G$  between a hard Key- and a hard (single cavity) Lock-particle has previously been shown to be<sup>1</sup>

$$\frac{\Delta G(r)}{k_B T} = \begin{cases} 0 & 0 \leq r < -(c - R_C + R_K) \\ 0 & R_L + R_K < r \\ -\ln\left(\frac{1 - \cos(\beta - \alpha)}{2}\right) & \text{otherwise.} \end{cases} \quad (\text{S1})$$

Here  $r = |\mathbf{r}| = |\mathbf{K} - \mathbf{L}|$ ,  $\alpha = \angle \mathbf{PLK}$  and  $\beta = \angle \mathbf{PLC}$ , where  $\mathbf{P}$  defines the contact point between the particles,  $k_B$  is the Boltzmann constant, and  $T$  is the temperature.

### S2.2 Multiple cavities

Now we simply extend the above presented expression to include multiple cavities. This is straight-forward as long as the cavities are mutually non-overlapping, and for the last case in Eq. S1 we get

$$\frac{\Delta G(r)}{k_B T} = -\ln\left(\sum_j \frac{1 - \cos(\beta_j - \alpha_j)}{2}\right) \quad (\text{S2})$$

where  $j$  index the different cavities. As an example, if a Lock-particle has  $X$  cavities all of equal size then the expression simplifies to

$$\frac{\Delta G(r)}{k_B T} = -\ln\left(X \frac{1 - \cos(\beta - \alpha)}{2}\right). \quad (\text{S3})$$

## S3 Electrostatic potential

For the electrostatics interactions between lock- and key-particles we use an approach for single-cavity lock-particles<sup>2</sup> but extend it to several cavities. The extension is solely based on describing the contributions from each cavity separately, and as they are treated separately all expressions in the original work<sup>2</sup> still applies. The main difference therefore is the division of space into regions, cf. Fig. S4 in reference<sup>2</sup> to our Fig. S1. As our approach treats the cavities separately, we assume the potential about one cavity to not heavily influence the others. This is a fair assumption for high ionic strengths which also is assumed in the derivation in the original work<sup>2</sup>.

<sup>a</sup> Physical Chemistry I, Center for Chemistry and Chemical Engineering, Lund University, 221 00 Lund, Sweden. E-mail: bjorn.stenqvist@teokem.lu.se

<sup>b</sup> Institute of Physical Chemistry, RWTH Aachen University, Landoltweg 2, 52074, Aachen, Germany. E-mail: crassous@pc.rwth-aachen.de

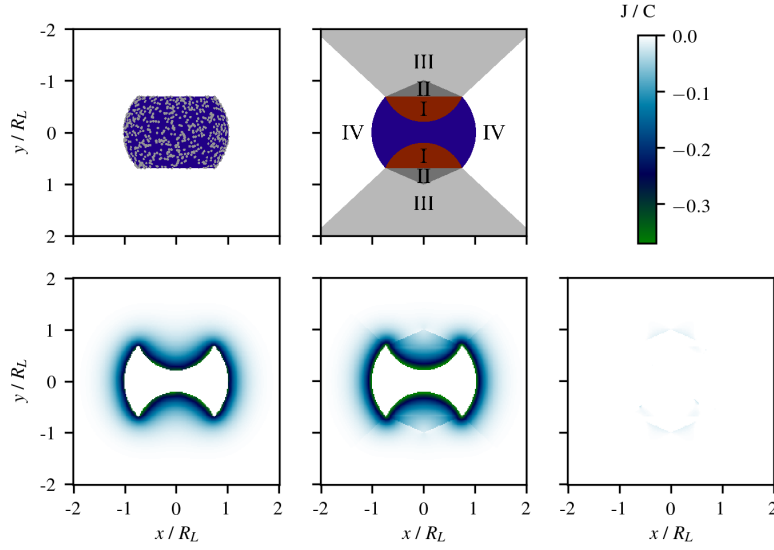


Figure S1 Potential from randomly distributed particles on the surface of a lock-particle (lower-left) and the approximate potential (lower-middle). The far right lower panel shows the difference between the two approaches. The screening for both figures was  $10^{-5}$  M. The upper figures illustrates the respective models and the regions.

### S3.1 Key-particle in front of Lock-particle cavity

Now we present the electrostatic Yukawa-potential  $V_L(z)$ , from a Lock-particle on the line parallel to  $\mathbf{c} = \mathbf{C} - \mathbf{L}$  going through  $\mathbf{L}$ , that is a straight line going through the center of the Lock-particle and one of its cavities. Eq. S9 is an analytic exact expression for the potentials on that line in front of the cavity. In Eq. S9  $q_L$  is the charge of the Lock-particle which is uniformly distributed on its surface-area  $A$  described in Eq S4. Also note that  $\kappa^{-1}$  is the Debye-length, that  $\angle \mathbf{RLC}$  and  $\angle \mathbf{RCL}$  are described in Eqs. S5-S6,  $\epsilon_0$  and  $\epsilon_r$  are the permittivity of vacuum and the relative permittivity of the dispersing medium respectively. Eq. S7 describes  $z$  as a function of the surface-to-surface distance  $d$  (see Eq. S8).

$$A = \frac{\pi}{c} (R_L^3 + (R_C + 2c)R_L^2 - (R_C^2 - c^2)R_L - (R_C - c)^2R_C) \quad (\text{S4})$$

$$\cos(\angle \mathbf{RLC}) = \frac{R_L^2 + c^2 - R_C^2}{2R_Lc} \quad (\text{S5})$$

$$\cos(\angle \mathbf{RCL}) = \frac{R_C^2 + c^2 - R_L^2}{2R_Cc} \quad (\text{S6})$$

$$z = \begin{cases} d + c - R_C & \forall z > c - R_C \\ -d - R_L & \forall z \leq -R_L \end{cases} \quad (\text{S7})$$

$$d(\mathbf{r}, \mathbf{c}) = \begin{cases} R_C - |\mathbf{r} - \mathbf{c}| - R_K & \text{Region I \& II} \\ |\mathbf{r}| - c + R_C - R_K & \text{Region III} \\ |\mathbf{r}| - R_L - R_K & \text{Region IV.} \end{cases} \quad (\text{S8})$$

There are now two special cases that needs considering:  $z = 0$  or  $z = c$ , where a denominator of Eq. S9 is zero. The first term in Eq. S9 using  $z \rightarrow 0$  results in the simplified Eq. S10 whereas the second term using  $z \rightarrow c$  is results in

Eq. S11.

$$\begin{aligned} \frac{V_L(z)}{\left(\frac{q_L}{4\pi\epsilon_0\epsilon_r}\right)} &= \frac{2R_L\pi}{A\kappa z} \left[ \exp\left(-\kappa\sqrt{R_L^2 - 2\cos(\angle\mathbf{RLC})R_L z + z^2}\right) - \exp(-\kappa|R_L + z|) \right] + \\ &+ \frac{2R_C\pi}{A\kappa(z-c)} \left[ \exp\left(-\kappa\sqrt{R_C^2 + 2\cos(\angle\mathbf{RCL})R_C(z-c) + (z-c)^2}\right) - \exp(-\kappa|R_C + z - c|) \right] \end{aligned} \quad (\text{S9})$$

$$\lim_{z \rightarrow 0} \frac{2R_L\pi}{A\kappa z} \left[ \exp\left(-\kappa\sqrt{R_L^2 - 2\cos(\angle\mathbf{RLC})R_L z + z^2}\right) - \exp(-\kappa|R_L + z|) \right] = \frac{2R_L\pi}{A} (\cos(\angle\mathbf{RLC}) + 1) e^{-\kappa R_L} \quad (\text{S10})$$

$$\lim_{z \rightarrow c} \frac{2R_C\pi}{A\kappa(z-c)} \left[ \exp\left(-\kappa\sqrt{R_C^2 + 2\cos(\angle\mathbf{RCL})R_C(z-c) + (z-c)^2}\right) - \exp(-\kappa|R_C + z - c|) \right] = -\frac{2R_C\pi}{A} (\cos(\angle\mathbf{RCL}) - 1) e^{-\kappa R_C} \quad (\text{S11})$$

As  $\kappa \rightarrow 0$  we use the asymptotic limit

$$\lim_{x \rightarrow 0} \left( \frac{e^{Ax} - e^{Bx}}{x} \right) = A - B \quad (\text{S12})$$

to get an accurate expression for the potential.

The interaction energy between a Lock- and a Key-particle is finally retrieved by using Eq. S9 and the effective charge of the Key-particle<sup>3,4</sup>,  $q_K^* = \frac{\sinh(\kappa R_K)}{\kappa R_K} q_K$ , where  $q_K$  is the charge of the Key-particle. Thus the interaction-energy is  $U_{LK}(z) = V_L(z)q_K^*$ .

### S3.2 Angular-dependent potential

The full angular-dependent potential is divided into four separate regions, see Fig. S1. In each region the potential is a linear combination of the potential derived in the previous subsection where the Key-particle is perfectly in front ( $V_L(z_{LK}(\mathbf{r}, \mathbf{c}))$ ) and behind ( $V_L(z_{LK}^-(\mathbf{r}, \mathbf{c}))$ ) the Lock-particle. Here

$$z_{LK}(\mathbf{r}, \mathbf{c}) = d(\mathbf{r}, \mathbf{c}) + c - R_C \quad (\text{S13})$$

and

$$z_{LK}^-(\mathbf{r}, \mathbf{c}) = -d(\mathbf{r}, \mathbf{c}) - R_L, \quad (\text{S14})$$

where the closeted distance to contact is described in Eq. S8. The potential is then described by

$$V_L(\mathbf{r}, \mathbf{c}) = \lambda(\mathbf{r}, \mathbf{c})V_L(z_{LK}(\mathbf{r}, \mathbf{c})) + (1 - \lambda(\mathbf{r}, \mathbf{c}))V_L(z_{LK}^-(\mathbf{r}, \mathbf{c})), \quad (\text{S15})$$

where  $\lambda(\mathbf{r}, \mathbf{c})$  is defined in the following. In Region I and Region III

$$\lambda_{\text{I}}(\mathbf{r}, \mathbf{c}) = \lambda_{\text{III}}(\mathbf{r}, \mathbf{c}) = \frac{\cos(\angle\mathbf{RCL}) - \cos(\angle\mathbf{LCK})}{\cos(\angle\mathbf{RCL}) - 1}, \quad (\text{S16})$$

in Region II

$$\lambda_{\text{II}}(\mathbf{r}, \mathbf{c}) = \frac{\cos(\angle\mathbf{RLC}) - \cos(\angle\mathbf{KLC})}{\cos(\angle\mathbf{RLC}) - 1}, \quad (\text{S17})$$

and ultimately in Region IV

$$\lambda_{\text{IV}}(\mathbf{r}, \mathbf{c}) = 0. \quad (\text{S18})$$

There is a single exception to the previous formulas, in Eq. S8, which is in  $z_{LK}^-(\mathbf{r}, \mathbf{c})$  in Region III where  $d =$

$\sqrt{R_L^2 + r^2 - 2R_L r \cos(\angle \mathbf{RLC} - \angle \mathbf{KLC})}$ , that is the closest distance to the rim of the Lock-particle.

This model was then compared to the aggregated potential from a random distribution of point charges, see Fig. S1

## S4 Derivation of number-ratios for assemblies

### S4.1 $L^2$ particles

#### S4.1.1 Chains

In a chain every other particle is a Lock and every other particle is a Key. Thus they each have two bonds with other particles. The total number of bonds can thus be described by

$$N_{\text{Tot.Bonds}} = 2N_L = 2N_K \quad (\text{S19})$$

which gives the number ratio

$$\frac{N_K}{N_L} = \frac{1}{1}. \quad (\text{S20})$$

#### S4.1.2 Diamond lattice

In the suggested diamond lattice every node is a Key and every bond between two such nodes are described by a Lock. The total number of bonds can thus be described in two ways by

$$N_{\text{Tot.Bonds}} = 2N_L = 4N_K \quad (\text{S21})$$

which gives the number ratio

$$\frac{N_K}{N_L} = \frac{1}{2}. \quad (\text{S22})$$

#### S4.1.3 Cubic lattice

In the suggested cubic lattice every node is a Key and every bond between two such nodes are described by a Lock. The total number of bonds can thus be described in two ways by

$$N_{\text{Tot.Bonds}} = 2N_L = 6N_K \quad (\text{S23})$$

which gives the number ratio

$$\frac{N_K}{N_L} = \frac{1}{3}. \quad (\text{S24})$$

### S4.2 $L^3$ particles - (2D)-hexagonal lattice

In the suggested (2D)-hexagonal lattice every node is a Lock and every bond between two such nodes are described by a Key. The total number of bonds can thus be described in two ways by

$$N_{\text{Tot.Bonds}} = 3N_L = 2N_K \quad (\text{S25})$$

which gives the number ratio

$$\frac{N_K}{N_L} = \frac{3}{2}. \quad (\text{S26})$$

### S4.3 $L^4$ particles - diamond lattice

In the suggested diamond lattice every node is a Lock and every bond between two such nodes are described by a Key. The total number of bonds can thus be described in two ways by

$$N_{\text{Tot.Bonds}} = 4N_L = 2N_K \quad (\text{S27})$$

which gives the number ratio

$$\frac{N_K}{N_L} = \frac{2}{1}. \quad (\text{S28})$$

#### S4.4 $L^6$ particles - cubic lattice

In the suggested cubic lattice every node is a Lock and every bond between two such nodes are described by a Key. The total number of bonds can thus be described in two ways by

$$N_{\text{Tot.Bonds}} = 6N_L = 2N_K \quad (\text{S29})$$

which gives the number ratio

$$\frac{N_K}{N_L} = \frac{3}{1}. \quad (\text{S30})$$

## S5 Excess of Lock-particles

In Fig. S2 we present typical configurations from simulations using different types of Lock- and Keys-particles, in an excess of the former. The clusters are connected with highly specific bonds yet they naturally display a lower degree of coordination between the satellites as compared to the opposite case of an excess of key-particles.

## S6 Free energy of binding

In Fig. S3 we present a lower limit of the free energy cost to form a cluster centered around a lock with the number of keys indexed in the legend. This latter number represent the average number of keys per lock in a perfect lattice. In the figure no electrostatics is accounted for. As already bound keys would prevent future bonds by their simple presence the true curves would be even higher than the ones displayed, more so for locks with several indentations than locks with fewer ones. The image indicate, from an entropic perspective, it to be more favourable to form clusters and lattices based on locks with few indentations to those of more cavities.

## S7 Simulation software

The simulation software is released under the GNU Public License and is available at:

<https://github.com/bjornstenqvist/beoFaunus>.

All code that has been used to produce results for this work is available there as well as an example setup for a simulation of lock and key particles.

## References

- 1 A. M. Mihut, B. Stenqvist, M. Lund, P. Schurtenberger and J. J. Crassous, *Sci. Adv.*, 2017, **3**, e1700321.
- 2 B. Stenqvist, M. Trulsson and J. J. Crassous, *Soft Matter*, 2019, **15**, 5234–5242.
- 3 B. Beresford-Smith, D. Y. Chan and D. J. Mitchell, *J. Colloid Interface Sci.*, 1985, **105**, 216–234.
- 4 R. Kjellander and D. J. Mitchell, *J. Chem. Phys.*, 1994, **101**, 603–626.

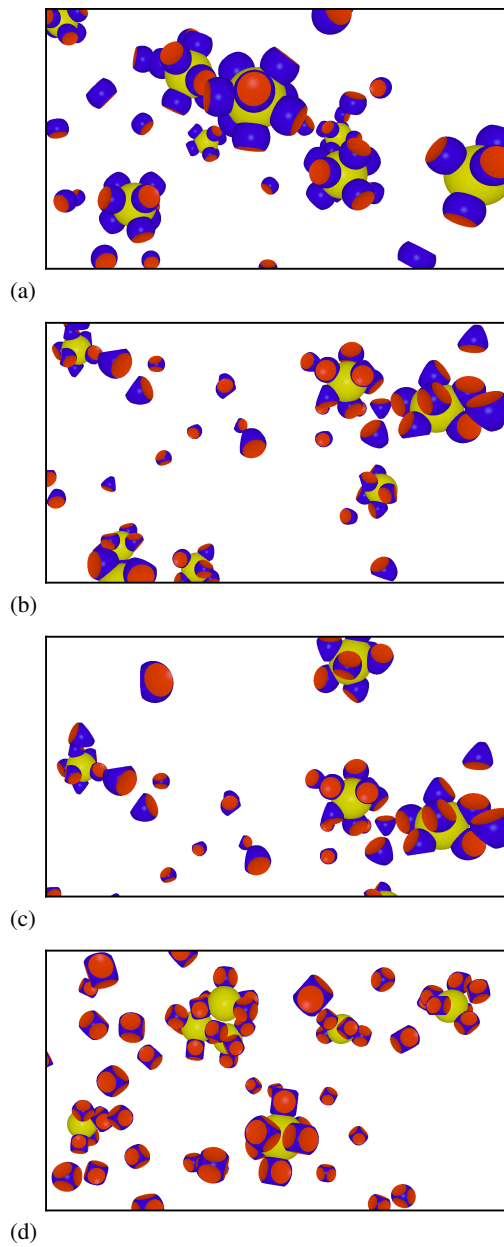


Figure S2 {(a),(b),(c),(d)} Typical configuration of key-particles in an excess of  $L^{\{2,3,4,6\}}$  particles using  $R_K = \{1.6, 1.6, 1.6, 1.4\}R_L$ ,  $c = 2.0R_L$ , and  $\sigma = 1.0\sigma_0$ .

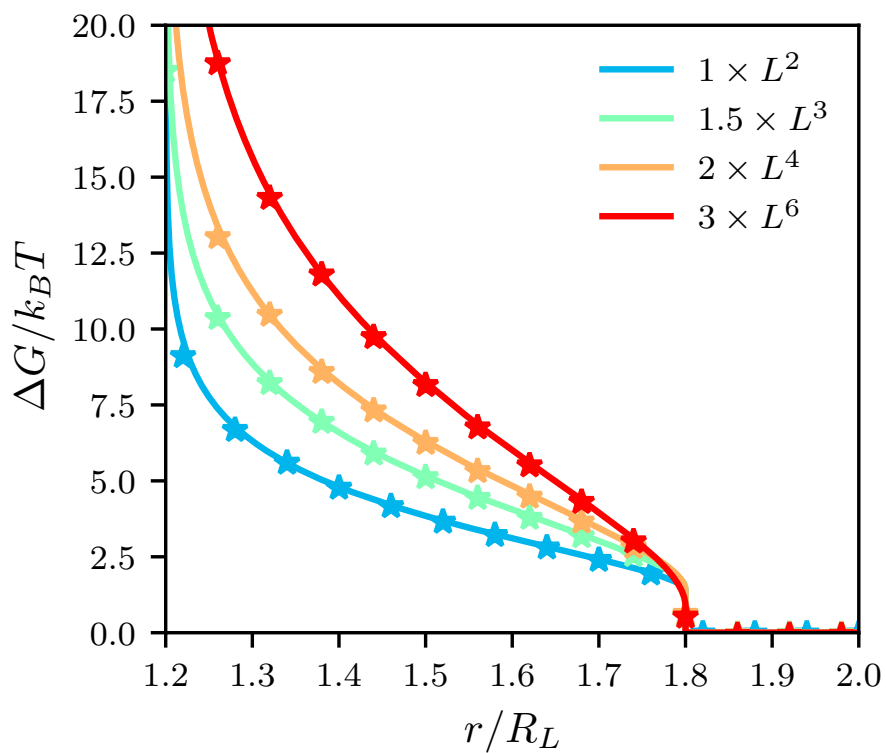


Figure S3 Analytic free energy (see Sec. S2) (lines) and simulation (stars) free energy between a lock- and a key-particle using a hard-overlap potential. The free energy is scaled by a factor indicated in the legend, which represent the average number of bound keys per lock in a perfect lattice. All cavities were located at  $c = 1.2R_L$  from the lock-particles center, where  $R_L$  is the lock radius. The radii of the cavities was  $R_C = R_K$ , where the key particle radius  $R_K = 0.8R_L$ .